

# Newtonian Dislocation Creep in Quartzites: Implications for the Rheology of the Lower Crust

J. N. Wang,\* B. E. Hobbs, A. Ord, T. Shimamoto, M. Toriumi

Mechanical and microstructural evidence indicates that a natural and a synthetic quartzite deformed by Newtonian dislocation (Harper-Dorn) creep at temperatures higher than 1073 K and stresses lower than 300 megapascals. The observation of this creep in these materials suggests that the lower crust may flow like a Newtonian viscous fluid by a dislocation mechanism at stresses much smaller than those previously postulated.

The dynamics of the lower crust are critically dependent on the plastic flow properties of its main constituent minerals. Quartz is one of them. Creep in many crystalline materials has been shown to change, as the applied stress,  $\sigma$ , decreases, from power law dislocation creep with a stress exponent,  $n$ , of 3 to 5 to Newtonian viscous flow with  $n = 1$ . The Newtonian behavior could be induced by diffusional creep involving the transfer of matter from one grain boundary to another (1) or by Harper-Dorn (H-D) creep, a Newtonian dislocation creep involving dislocation activation within grains (2). This change, however, had not been observed in quartz, despite extensive studies. The lack of knowledge about this change has prevented accurate modeling of the deformation on various scales, ranging from minor folding to plate tectonic boundaries, as well as reliable reconstruction of the thermomechanical history of the lower crust. We report here experimental evidence for the operation of Newtonian dislocation creep in a natural quartzite and suggest that it was also seen in deformation of a synthetic quartzite in an earlier study (3).

We conducted creep experiments in a solid confining-medium, Tullis-modified, Griggs rig on Heavittree quartzite. This almost undeformed starting material contained only small amounts (<2%) of impurities (feldspar, mica, and iron oxides) and had a grain size,  $d$ , of  $200 \pm 50 \mu\text{m}$  (4). The specimen assembly used was the same as that in (5). All specimens were deformed at constant differential stresses,  $\sigma$ , of 100 to 1000 MPa; constant temperatures,  $T$ , of 873 to 1173 K; and a nominal confining pressure,  $P_c$ , of 1500 MPa. Before the start of

deformation, specimens were held at experimental  $T$  and  $P_c$  for 20 hours. Increase in the cross-sectional area of the specimen with strain was compensated by increasing the axial load gradually with computer interfacing. We controlled oxygen, water, and hydrogen fugacities ( $f_{\text{O}_2}$ ,  $f_{\text{H}_2\text{O}}$ , and  $f_{\text{H}_2}$ ) in the environment (4) by enclosing the specimen with a small amount of a solid oxygen buffer ( $\sim 0.25 \text{ mg}$ ) and water ( $\sim 50 \mu\text{l}$ ) in a mechanically sealed Ag capsule. Oxygen buffers used were  $\text{Mn}_3\text{O}_4/\text{Mn}_2\text{O}_3$ ,  $\text{Cu}/\text{Cu}_2\text{O}$ ,  $\text{Ni}/\text{NiO}$ ,  $\text{Mo}/\text{MoO}_2$ , and  $\text{Ta}/\text{Ta}_2\text{O}_5$ , which covered wide ranges of fugacities.

A mechanical steady state was reached after 3 to 5% strains and continued to high strains ( $\sim 50\%$ ) in most of the experiments. The creep rate in this state,  $\dot{\epsilon}$ , increased with increasing  $\sigma$ ,  $T$ ,  $f_{\text{O}_2}$ , and  $f_{\text{H}_2\text{O}}$ . Two distinct creep regimes were observed at  $T > 973 \text{ K}$  in all buffered environments, one at  $\sigma \leq 300 \text{ MPa}$  with  $n \approx 1$  and the other at  $\sigma \geq 500 \text{ MPa}$  with  $n \approx 2.4$  (Fig. 1). We used the following form of the flow law to fit creep data falling in different regimes separately:

$$\dot{\epsilon} = A(f_{\text{O}_2})^m(f_{\text{H}_2\text{O}})^p \sigma^n \exp\left(-\frac{Q}{RT}\right) \quad (1)$$

where  $A$  is a material constant,  $Q$  is the activation energy,  $R$  is the gas constant, and  $m$  and  $p$  are fugacity exponents. The best

fitting results are, for the  $n = 1$  regime,  $A = 1.57 \times 10^{-3} \text{ s}^{-1} \text{ MPa}^{-m-p-n}$  with  $m \approx 0$ ,  $p = 0.41$ , and  $n = 0.99$ , and  $Q = 131.5 \text{ kJ/mol}$ ; and, for the  $n \approx 2.4$  regime,  $A = 9.14 \times 10^{-8} \text{ s}^{-1} \text{ MPa}^{-m-p-n}$  with  $m \approx 0$ ,  $p = 0.24$ ,  $n = 2.39$ , and  $Q = 101.3 \text{ kJ/mol}$ .

The optical microstructures observed in both regimes of  $n = 1$  and  $n = 2.4$  were homogeneously flattened grains, deformation lamellae, subgrains, new recrystallized quartz crystals, and small amounts of melt (1% by volume in Ta-buffered specimens and 3% by volume in Mn-buffered specimens) (6). Transmission electron microscopy (TEM) observations showed that the deformation lamellae in the  $n = 1$  regime were parallel dislocation arrays but that those in the  $n = 2.4$  regime were strips with intensely tangled dislocations. Most recrystallized grains originating from subgrain rotation and grain-boundary migration in the  $n = 2.4$  regime were so small that they could not be easily identified without TEM. The melt tended to reside at triple grain junctions and grain boundaries oriented at the loading direction.

The most remarkable microstructural difference between the two regimes was that, in the  $n = 1$  regime, free dislocations were generally curved, long, and homogeneously distributed in the interiors of original grains or subgrains. Many bowed toward the same direction, which indicated their moving orientation. However, in the  $n = 2.4$  regime, curved free dislocations were short whereas straight free dislocations found in some grains were long and strongly crystallographically controlled. Such crystallographically controlled dislocations, which suggest the occurrence of pure glide, were never observed in the  $n = 1$  regime. Another difference between the two regimes was that the free dislocation density did not change with changing stress in the  $n = 1$  regime ( $\sim 5 \times 10^{13} \text{ m}^{-2}$ ), although it did increase with in-

J. N. Wang and T. Shimamoto, Earthquake Research Institute, University of Tokyo, Bunkyo-ku, Tokyo, 113, Japan.

B. E. Hobbs and A. Ord, Commonwealth Scientific and Industrial Research Organization, Division of Exploration and Mining, Post Office Box Wembley, WA 6014, Australia.

M. Toriumi, Geological Institute, University of Tokyo, Bunkyo-ku, Tokyo, 113, Japan.

\*Present address: Chemistry and Materials Science, L-370, Lawrence Livermore National Laboratory, Post Office Box 808, Livermore, CA 94450, USA.

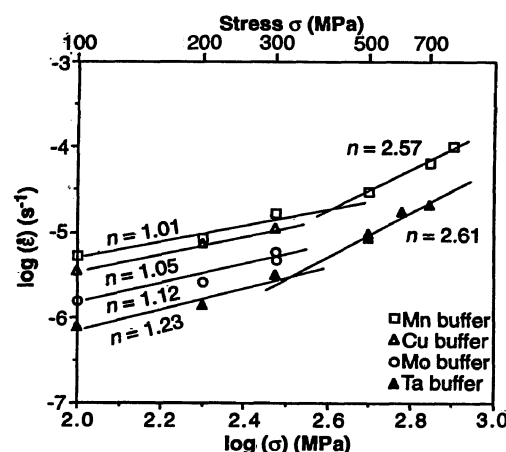


Fig. 1. Plot of creep data for natural quartzite at  $T = 1073 \text{ K}$ . A regime of  $n = 1$  is exhibited in all buffered environments at low stresses.

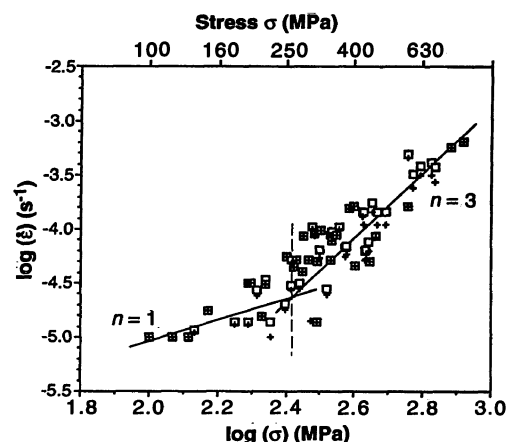


Fig. 2. Plot of the original (+) and the recalculated (□) rheological data from (3) for the silica gel-origin quartzite at  $T = 1300 \text{ K}$ . Both sets of data show a regime of  $n = 1$  at  $\sigma < 260 \text{ MPa}$ .

creasing stress in the  $n = 2.4$  regime (6).

For partial melting to have a significant effect on the rheology of the bulk specimen, the melt phase must totally intrude into all grain boundaries or form an interconnected, three-dimensional network along three-grain edge intersections (7). The presence of small amounts of melt residing at triple grain junctions in the  $n = 1$  regime is unlikely to provide a short circuit diffusion path and thus enhance grain boundary diffusional creep (8). The strong grain flattening and the extensive formation of dislocation-related microstructures, together with the obvious development of  $c$  axis preferred orientations in the  $n = 1$  regime (6), are inconsistent with deformation by diffusional or grain boundary sliding creep but suggest control of an intragranular dislocation process operating in H-D creep.

In a similar study, Luan and Paterson (3) compressed synthetic quartzites at a constant piston displacement rate and at  $T = 1100$  to  $1500$  K and  $P_c = 300$  MPa. They found a stress exponent,  $n$ , of  $\sim 2.3$  for gel-origin specimens and an  $n$  of  $\sim 4$  for silicic acid-origin specimens, regardless of the stress level. However, the reported  $n$  values may not be accurate. The apparent strain rate ( $\dot{\epsilon}_p$ ) reported in (3) was calculated from an imposed constant displacement rate and the original specimen length. Such  $\dot{\epsilon}_p$  underestimates the true strain rate ( $\dot{\epsilon}$ ) at the true flow stress based on the current cross-sectional area of the specimen. The underestimation becomes nonnegligible if the specimen is shortened by more than 10% strain. If the current true strain is  $\epsilon$ , then

$$\dot{\epsilon} = \dot{\epsilon}_p \exp(\epsilon) \quad (2)$$

In a majority of the original experiments of Luan and Paterson, displacement rate, temperature, or both were stepped to different levels. In each step, the specimen was deformed generally for less than 10% strain. We recalculated all reported  $\dot{\epsilon}_p$  data to  $\dot{\epsilon}$  using Eq. 2, taking  $\epsilon$  as the true strain at the start of each step. The revised  $\dot{\epsilon}$ - $\sigma$  data on the gel-origin specimens from (3) (Fig. 2)

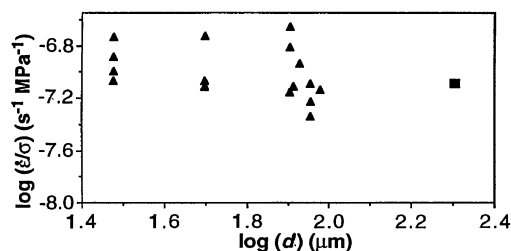


**Fig. 3.** Illustration of the independence of the Newtonian creep with respect to grain size, based on the recalculated data for the gel-origin quartzite from (3) (▲). The present data (■) for Heavitree quartzite with  $d \approx 200$   $\mu\text{m}$  were adjusted to  $T = 1300$  K and  $f_{\text{H}_2\text{O}} = 300$  MPa (Eq. 1) ( $n = 1$ ) and are included for comparison.

show two rheological regimes, one with  $n \approx 1$  and the other with  $n \approx 3$ , with the division occurring at  $\sigma \approx 260$  MPa (9). This division could also be seen in the original data.

To investigate grain size effect, we examined the recalculated data of different grain sizes from (3) at  $\sigma < 260$  MPa in the form of  $\log(\dot{\epsilon}/\sigma)$  versus  $\log(d)$  (Fig. 3) and observed that the Newtonian creep of the gel-origin synthetic quartzite is independent of  $d$  in the experimental grain size range of 30 to 100  $\mu\text{m}$ . This Newtonian creep behavior is inconsistent with existing diffusional or grain boundary sliding creep mechanisms, which show grain size dependencies, but is in agreement with H-D creep, which involves intragranular dislocation motion and thus is not affected by the grain size.

In contrast to the specimens of gel origin, the recalculated data from (3) for the quartzite of silicic acid origin yield  $n \approx 3$  at all experimental stresses. Failure to observe H-D creep in this material may be related to its low water concentration (10).

Natural quartzites were also deformed to a mechanical steady state in some other studies (11). However, Newtonian creep behavior was not observed. Although it is impossible to explain fully the differences between the previous and the present results, we suggest that application of a constant stress (rather than a constant load) or a constant strain rate (rather than a constant displacement rate), a high water concentration in the starting material (10), and sufficient heat treatment before loading (12) might be important for the observation of H-D creep.

The stress marking the transition from power law creep ( $n = 2.4$  or 3) to H-D

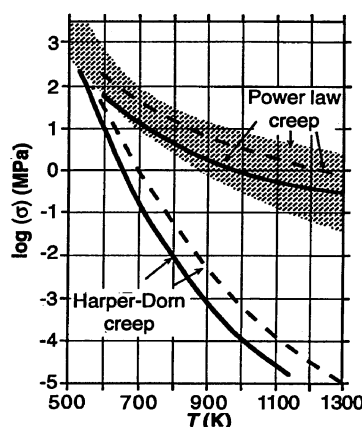


**Fig. 4.** Extrapolation of the flow laws for H-D creep and power law creep for the present natural (solid heavy lines) and the silica gel-origin synthetic (3) (dashed heavy lines) quartzites to a geological strain rate of  $10^{-12}$   $\text{s}^{-1}$  at  $f_{\text{H}_2\text{O}} \approx 300$  MPa. The hatched region represents earlier results also on quartzites for power law creep summarized by Paterson and Luan (15).

creep,  $\sigma_c$ , is  $\sim 260$  to 300 MPa in synthetic and natural quartzites. The dislocation density in H-D creep,  $\rho$ , is  $\sim 5 \times 10^{13}$   $\text{m}^{-2}$  for quartzite. These values of  $\sigma_c$  and  $\rho$  are significantly larger than those observed for metals ( $\sigma_c < 1$  MPa,  $\rho \approx 10^8$   $\text{m}^{-2}$ ) and oxides ( $\sigma_c < 100$  MPa). These differences may be due to the fact that quartz has a higher Peierls stress than the latter materials (13).

The rheology of the lower crust is generally believed to be determined by the flow behavior of quartz and feldspar. Observation of H-D creep in quartzites, and in both a single crystal and a polycrystal of feldspar (14), indicates that the lower crust flows like a Newtonian viscous fluid by a dislocation mechanism. By extrapolating the determined flow laws of H-D creep and those of power law creep for quartzites to the conditions in the lower crust (Fig. 4), we found that, at a geological strain rate of  $10^{-12}$   $\text{s}^{-1}$  and temperature of 773 K, the flow stress of quartzite controlled by H-D creep is smaller by more than two orders of magnitude than that controlled by power law creep. This result indicates that the stress level in the lower crust, if H-D creep is rate-controlling, may be significantly smaller than that believed previously (11, 15), assuming that power law creep is rate-controlling.

## REFERENCES AND NOTES

1. F. R. N. Nabarro, in *Report of a Conference on Strength of Solids* (University of Bristol) (Physical Society, London, 1948), pp. 75–90; C. Herring, *J. Appl. Phys.* **21**, 437 (1950); R. L. Coble, *ibid.* **34**, 1679 (1963).
2. J. C. Harper and J. E. Dorn, *Acta Metall.* **5**, 654 (1957).
3. F. C. Luan and M. S. Paterson, *J. Geophys. Res.* **97**, 301 (1992).
4. J. N. Wang, J. N. Boland, A. Ord, B. E. Hobbs, in *Defects and Processes in the Solid State: Geoscience Application (The McLaren Volume)*, J. N. Boland and J. Fitz Gerald, Eds. (Elsevier, Amsterdam, 1993), pp. 359–381.
5. A. Ord and B. E. Hobbs, in *Mineral and Rock Deformation: Laboratory Studies (The Paterson Volume)*, B. E. Hobbs and H. C. Heard, Eds. (American Geophysical Union, Washington, DC, 1986), pp. 51–72.
6. J. N. Wang, thesis, Monash University, Melbourne, Australia (1992); ———, B. E. Hobbs, A. Ord, J. N. Boland, unpublished results.
7. T. J. Shankland, R. J. O'Connell, H. S. Waff, *Rev. Geophys.* **19**, 394 (1981); R. F. Cooper, *J. Geophys. Res.* **95**, 6979 (1990).
8. R. F. Cooper and D. L. Kohlstedt, *J. Geophys. Res.* **91**, 9315 (1986); L. N. Dell'Angelo and J. Tullis, *J. Metamorph. Geol.* **6**, 495 (1988); B. R. Hacker and J. M. Christie, *Tectonophysics* **200**, 79 (1991); M. L. Beeman and D. L. Kohlstedt, *J. Geophys. Res.* **98**, 6443 (1993).
9. We adjusted several datum points from  $T$  of between 1100 and 1250 to 1300 K, using the originally reported and also newly determined  $Q$  of 150 kJ/mol. With the observed  $n$  and  $Q$  values, the value of  $A'$  in the flow law of
 
$$\dot{\epsilon} = A' \sigma^n \exp(-Q/RT)$$
 is 0.11  $\text{s}^{-1} \text{MPa}^{-1}$  for the  $n \approx 1$  regime and  $1.86 \times 10^{-6} \text{s}^{-1} \text{MPa}^{-3}$  for the  $n \approx 3$  regime.
10. J. N. Wang and T. G. Langdon [*Acta Metall.* **42**,

2487 (1994)] demonstrated that the rate-controlling flow process in H-D creep is the climb of dislocations saturated with vacancies. The incorporation of water into quartz structure enhances the concentration of O or Si vacancies, depending on the neutrality condition [B. E. Hobbs, in *Point Defects in Minerals*, R. N. Schock, Ed. (American Geophysical Union, Washington, DC, 1985), pp. 151–170]. Thus, dislocations might be saturated in the gel-origin quartzite with high water concentrations ( $> 5500$  H per  $10^6$  Si) but might not be saturated in the silicic acid-origin quartzite, which has low water concentrations (generally much lower than  $4500$  H per  $10^6$  Si).

11. P. S. Koch, J. M. Christie, A. Ord, R. P. George Jr., *J. Geophys. Res.* **94**, 13975 (1989); A. K. Kronenberg and J. Tullis, *ibid.* **89**, 4281 (1984); O. Jaoul, J. Tullis, A. K. Kronenberg, *ibid.*, p. 4298.
12. F. A. Mohamed and T. J. Ginter [*Acta Metall.* **30**, 1869 (1982)] showed that H-D creep would not be observed in Al specimens unless the dislocation density in the sample before loading was sufficiently low. This result indicates that there might be a substructural requirement for the occurrence of H-D creep.
13. J. N. Wang, *Scr. Metall.* **29**, 733 (1993); *ibid.*, p. 1505; *Philos. Mag. A*, in press.
14. ——— and M. Toriumi, *Mater. Sci. Eng.*, in press.

15. M. S. Paterson and F. C. Luan, in *Deformation Mechanisms, Rheology, and Tectonophysics*, R. J. Knipe and E. H. Rutter, Eds. (Geological Society Special Publication 54, London, 1990), pp. 299–307.
16. Postdoctoral support for J.N.W. was provided by the Japan Society for the Promotion of Science. J. N. W. thanks J. N. Boland for instructing some TEM work and many people (especially S. He) in Central South University of Technology, Changsha, for valuable discussion. Comments by J. Tullis improved the report.

11 January 1994; accepted 29 June 1994

## The Nature of the Glass Transition in a Silica-Rich Oxide Melt

Ian Farnan\* and Jonathan F. Stebbins†

The atomic-scale dynamics of the glass-to-liquid transition are, in general, poorly understood in inorganic materials. Here, two-dimensional magic angle spinning nuclear magnetic resonance spectra collected just above the glass transition of  $K_2Si_4O_9$  at temperatures as high as  $583^\circ\text{C}$  are presented. Rates of exchange for silicon among silicate species, which involves Si–O bond breaking, have been measured and are shown to be closely related in time scale to those defined by viscosity. Thus, even at viscosities as high as  $10^{10}$  pascal seconds, local bond breaking (in contrast to the cooperative motion of large clusters) is of major importance in the control of macroscopic flow and diffusion.

Molten silicates play a major role in heat and mass transfer in the crust and mantle of the Earth, as well as being the precursors to technological materials such as glass and ceramics. If crystal nucleation and growth rates are slow in comparison to the rate of temperature decrease, cooling of a silicate liquid will result in its transformation to a glass at a rate-dependent temperature  $T_g$ . This transition is generally marked by substantial decreases in heat capacity, thermal expansivity, and compressibility that reach values in the glass that are similar to those of the corresponding crystalline solid. The glass transition is traditionally viewed as the temperature at which the rate of change of the structure of the liquid with cooling ( $\alpha$  structural relaxation) becomes too slow to remain in equilibrium at the given cooling rate. More rapid  $\beta$  processes, while of relatively minor bulk energetic consequence in silicates, may contribute to ultrasonic and dielectric relaxation both above and even well below  $T_g$  (1). The uncoupling of  $\alpha$  processes from  $\beta$  processes during cooling may be an important part of the transition from liquid to glass (2).

The configurational entropy generated by structural change above  $T_g$  is quantitatively linked to viscosity (3). An under-

standing of the structural mechanism of the transition to a glass can thus provide insights into both thermodynamic and transport properties of the liquids, as well as the relaxation that takes place during annealing of glasses, which transforms them into usable materials. In this report, we describe two-dimensional (2D)  $^{29}\text{Si}$  magic angle spinning nuclear magnetic resonance (MAS-NMR) experiments on  $K_2Si_4O_9$  liquid at temperatures just above  $T_g$  that provide a new quantitative link between bulk viscosity and a microscopic mechanism of exchange among structural species.

As a liquid,  $K_2Si_4O_9$  consists of a network of  $SiO_4$  tetrahedra, with some relatively large sites occupied by network-modifying  $K^+$  cations. In about half of the tetrahedra ( $Q^4$  groups), all four oxygens are linked to other tetrahedra (bridging oxygens); in the other half ( $Q^3$  species), one oxygen is not shared by a second Si but is coordinated by several  $K^+$  cations (nonbridging oxygens). A variety of minor species are also present, including  $SiO_5$  groups (4). At normal laboratory cooling rates,  $T_g$  for this liquid is close to  $500^\circ\text{C}$  (5). In previous one-dimensional (1D) static (non-MAS)  $^{29}\text{Si}$  NMR work at higher temperatures (6), the presence of a single resonance line indicated rapid chemical exchange of silicon between  $Q^3$  and  $Q^4$  groups. The measured rates at which these species exchange with each other, and also the rate at which bridging and nonbridging oxygens exchange, was used in a simple model to

accurately predict the bulk viscosity down to about  $850^\circ\text{C}$  (6, 7).

A possible mechanism for this process, which is consistent with a number of published molecular dynamics simulations, is shown in Fig. 1. At these higher temperatures this two-step exchange process passes easily through the intermediate step to complete exchange from  $Q^3$  to  $Q^4$ . The NMR exchange rate data could also be collected down to  $690^\circ\text{C}$ , but in this lower range, predicted viscosities were significantly lower than experimental values. This divergence is probably a result of the progressive inhibition of complete exchange and the increased importance of self-exchange to 1D NMR line narrowing. Formation of the intermediate state (Fig. 1) followed by decay back to original  $Q^3$  and  $Q^4$  species without exchange but with changed orientations with respect to the external magnetic field will contribute to 1D NMR peak narrowing but not to the flow mechanism of the liquid because there is no net throughgoing motion of an oxide anion. The 1D NMR spectra are limited because they are sensitive only to motions with frequencies within about an order of magnitude of the frequency separation and widths (in hertz) of their component peaks. For the static  $^{29}\text{Si}$  NMR spectrum of  $K_2Si_4O_9$ , this is  $\sim 10$  kHz, and the slowest motions that could be detected were thus about 1 kHz.

In contrast, 2D chemical exchange NMR experiments can detect much slower motions and can also separate the complete exchange from other peak-narrowing processes. This approach has been developed and elegantly applied to quantify dynamics in organic polymers, including studies of the nature of the glass transition (8,9). The technique has been described in detail (10) and involves a typical 2D NMR sequence of preparation, evolution, mixing, and detection. The 2D Fourier transform produced at the end of the experiment displays correlations between the NMR frequency of a nucleus at the start and at the end of the mixing time. The mixing time ( $t_{\text{mix}}$ ) is chosen to probe characteristic times associated with exchange in the sample, and observable dynamics are thus not limited by

Department of Geological and Environmental Sciences, Stanford University, Stanford, CA 94305, USA.

\*Present address: Centre de Recherches sur la Physique des Hautes Températures, Conseil National de Recherche Scientifique, 45071 Orléans Cedex 2, France.

†To whom correspondence should be addressed.